

Overwriting of sedimentary magnetism by bacterially mediated mineral alteration

Yael Ebert^{1*}, Ron Shaar¹, Simon Emmanuel¹, Norbert Nowaczyk², and Mordechai Stein^{1,3}

¹The Institute of Earth Sciences, The Hebrew University of Jerusalem, Jerusalem 91904, Israel

ABSTRACT

Marine and lacustrine sediments represent an important source of global paleomagnetic data. Although it is usually assumed that detrital iron oxides record most of the magnetic signal in sediments, iron sulfides-which form during bacterial sulfate reduction-can also represent a significant source of sedimentary magnetism. Knowing how sulfate reduction impacts sedimentary magnetism is critical to the interpretation of paleomagnetic records. Here, we show that three distinct types of magnetic particles can be produced by bacterial sulfate reduction, each of which impacts the bulk sediment magnetism in a distinct way. We combined magnetic force microscopy and electron probe microanalysis to image magnetic mineral extracts from Dead Sea sediments from a glacial period and an interglacial period. In sediments from the dry interglacial period, during which bacterial sulfate reduction was suppressed, we found greigite framboids (Fe₃S₄) with strong intergrain magnetic interactions. Contrastingly, in sediments from the wet glacial period, which experienced extensive sulfate reduction, pyrite (FeS₂) is the dominant sulfide phase. Highresolution magnetic imaging of glacial pyrite reveals that greigite is present as single-domain particles within the pyrite. We also found that as titanomagnetite grains undergo bacterially mediated alteration to form pyrite, the original magnetic grains become divided into smaller regions, which potentially facilitates acquisition of secondary magnetization by the reorganization of these magnetic domains. Our results provide a previously undocumented mechanism by which bacterially mediated alteration can overwrite primary detrital magnetic records.

INTRODUCTION

Paleomagnetic data from lacustrine and marine sediments are commonly used for dating and reconstructing depositional conditions. Although it is usually assumed that detrital iron oxides record most of the magnetic signal in the sediments, iron sulfides, which form during bacterial sulfate reduction or during anaerobic oxidation of methane, can also provide a significant source of sedimentary magnetism (Roberts and Turner, 1993; Roberts and Weaver, 2005; Roberts, 2015). Thus, knowing how these processes impact sedimentary magnetism is critical for interpreting paleomagnetic records.

The magnetic information recorded in sediments is influenced strongly by the way in which the magnetic signal is acquired, and the type of magnetic minerals present. Two processes are typically considered to dominate the magnetic signal of sediments: (1) depositional magnetization, which is acquired as detrital ferrimagnetic minerals become aligned during or after settling and deposition, and (2) chemical magnetization, which is acquired as authigenic ferrimagnetic minerals form within the sediment. Distinguishing between these processes is often a challenging task, especially in

environments where sulfate reduction and anaerobic oxidation of methane occur. In such environments, microbial activity triggers a complicated interplay between acquisition of a primary depositional magnetization by detrital magnetic minerals, dissolution of magnetite, and acquisition of chemical magnetization by authigenic greigite (Fe₃S₄) (Roberts et al., 2011; Roberts and Weaver, 2005; Ron et al., 2006; Rowan et al., 2009).

Ferrimagnetic greigite has been shown to have a strong influence on the magnetic properties of sediments (Roberts et al., 2011, and references therein; Ron et al., 2006; Sagnotti and Winkler, 1999). Although greigite forms in sediments, it is thermodynamically metastable and transforms to paramagnetic pyrite (FeS₂) (Hunger and Benning, 2007). As a result, in sulfate-reducing environments, which promote pyrite formation, greigite is sometimes thought to be absent or to appear in negligible amounts (Berner, 1984), and thus has no effect on the magnetic signal. Curiously, pyrite is often present in magnetic extracts from such sediments (Nowaczyk, 2011; Roberts and Turner, 1993; Rowan and Roberts, 2006), indicating that it must also contain a ferrimagnetic phase. To determine the impact of varying degrees of bacterial sulfate reduction on iron sulfide mineralogy and magnetism, we analyzed sediments that were deposited under distinct limnological conditions (e.g., meromictic vs. holomictic lakes) in lakes that filled during the late Quaternary in the Dead Sea basin.

GEOLOGICAL AND LIMNOLOGICAL SETTING

Located between Jordan and Israel, the modern Dead Sea is a hypersaline terminal lake that evolved from former lakes that filled the tectonic depression of the Dead Sea basin during the Quaternary (Stein, 2001). The lakes rose and expanded during wetter glacial intervals, and they dropped and contracted during drier interglacial periods (Bartov et al., 2003; Torfstein et al., 2013). The highstand lakes during glacials were characterized by layered, meromictic configuration, while the lakes typically overturned during the interglacials, forming a holomictic water body. The lakes are filled by calcium-chloride (CaCl₂) brine that has been mixed during the history of the lakes with freshwater from the large Dead Sea watershed. The freshwater supplies sulfate to the CaCl, brine (see Stein et al., 1997). Changes in freshwater input to the Dead Sea between interglacial and glacial periods impact the activity of sulfate-reducing bacteria (Thomas et al., 2016; Torfstein et al., 2005). A large input of freshwater dilutes the epilimnion (upper layer of water in a stratified lake), replenishes the lake with sulfate, and promotes the bloom of halophilic algae, which are the main source of organic matter input to the sediment (Oren et al., 1995; Torfstein et al., 2005). Hence, during wet glacial periods, pyrite is produced and preserved in the sediment, while during dry periods, greigite is preserved extensively (Thomas et al., 2016).

METHODS

Magnetic extracts were isolated from sediments of two lacustrine formations that represent distinct limnological settings in the history of the Dead Sea: the Lisan Formation (last glacial period ca. 70–14 ka), deposited

²Helmholtz Centre Potsdam, GFZ German Research Centre for Geosciences, 14473 Potsdam, Germany

³Geological Survey of Israel, Jerusalem 95501, Israel

^{*}E-mail: yael.ebert@mail.huji.ac.il

in a highstand meromictic lake, and the Ze'elim Formation (Holocene), deposited in a lowstand holomictic lake. The sediments were collected from cores drilled in the deepest floor of the Dead Sea by the International Continental Scientific Drilling Program (ICDP; Neugebauer et al., 2014). Magnetic minerals were extracted from a mixture of 2–3 cm³ of sediment and alcohol, using a strong hand magnet within a plastic probe (Nowaczyk, 2011). The extracts were embedded in epoxy for electron and magnetic microscopy, and polished down to 0.04 μm using colloidal silica.

Mineral composition was analyzed using a JEOL 8230 superprobe electron microprobe equipped with an energy dispersive X-ray spectroscopy (EDS) detector and four wavelength-dispersive spectrometers (WDS) at the Institute of Earth Sciences (IES), The Hebrew University of Jerusalem. Beam conditions were set to 15 keV and 15 nA for EDS and WDS analyses, with an excitation volume of 2 μm^3 , and 15 keV and 50 nA for WDS mapping, with an excitation volume of 0.5 μm^3 . All phases were analyzed for Ti, Fe, S, and O using hematite and pyrite standards. Data were processed with a PRZ correction procedure.

Magnetic force microscopy (MFM) was carried out using a Veeco Multimode 8 atomic force microscope (AFM) with a NanoScope V controller and NanoScope 8.15 software at the IES. In a magnetic mode of operation, a vibrating cantilever with a sharp magnetized tip was used to scan the sample twice. In the first scan, the tip tapped on the sample surface and measured the surface topography at the nanometer scale. In the second scan, the tip was maintained at a constant height above the sample and measured the net magnetic field originating from the magnetic minerals by sensing changes in the amplitude and phase of the vibrating cantilever. The color map in the MFM phase image is a qualitative view of the relative intensity of the magnetic field above the sample. The contrast between dark and light zones indicates different directions of the magnetic field, while neutral color represents nonmagnetic areas. Patterns of light and dark areas in a particle can be interpreted as different magnetic structures (de Groot et al., 2014; Pokhil and Moskowitz, 1997; Shaar and Feinberg, 2013).

An isothermal remanent magnetization (IRM) was imparted using an ASC pulse magnetizer with a 1.5 T field. First-order reversal curves (FORCs) were measured using a Princeton Measurements vibrating sample magnetometer at the Institute for Rock Magnetism, University of Minnesota (Minneapolis, Minnesota, USA).

RESULTS

Three types of magnetic mineral grains were identified: multidomain, noninteracting single domain, and interacting particles ("superstate"). Each of these distinct grain types contributes differently to the bulk sedimentary magnetic properties.

Of the three magnetic grains types, detrital titanomagnetite [Fe²⁺(Fe³⁺,Ti)₂O₄] is present in both Holocene (Ze'elim Formation) and last glacial (Lisan Formation) samples. The titanomagnetite grains are generally tens of micrometers in size, and while some are idiomorphic and well preserved, others have been partially or completely replaced by secondary phases, such as pyrite and greigite (as shown by Canfield and Berner, 1987). The large size of the titanomagnetite grains indicates that they are in the multidomain range (Muxworthy and Williams, 2006). The effect of bacterially facilitated replacement by pyrite of a titanomagnetite grain on the magnetic signal of detrital grains can be observed in MFM images (Fig. 1). An initially complete multidomain titanomagnetite grain potentially carrying primary detrital magnetization (Figs. 1A and 1B) differs from those that have been divided into smaller regions during mineral replacement (Figs. 1C-1F). The light and dark stripes in the MFM image of these regions are typical of patterns reported in multidomain grains (de Groot et al., 2014; Pokhil and Moskowitz, 1997; Shaar and Feinberg, 2013). Importantly, the walls of the multiple domains in each region must realign during the mineral alteration process, triggering acquisition of a secondary magnetic signal.

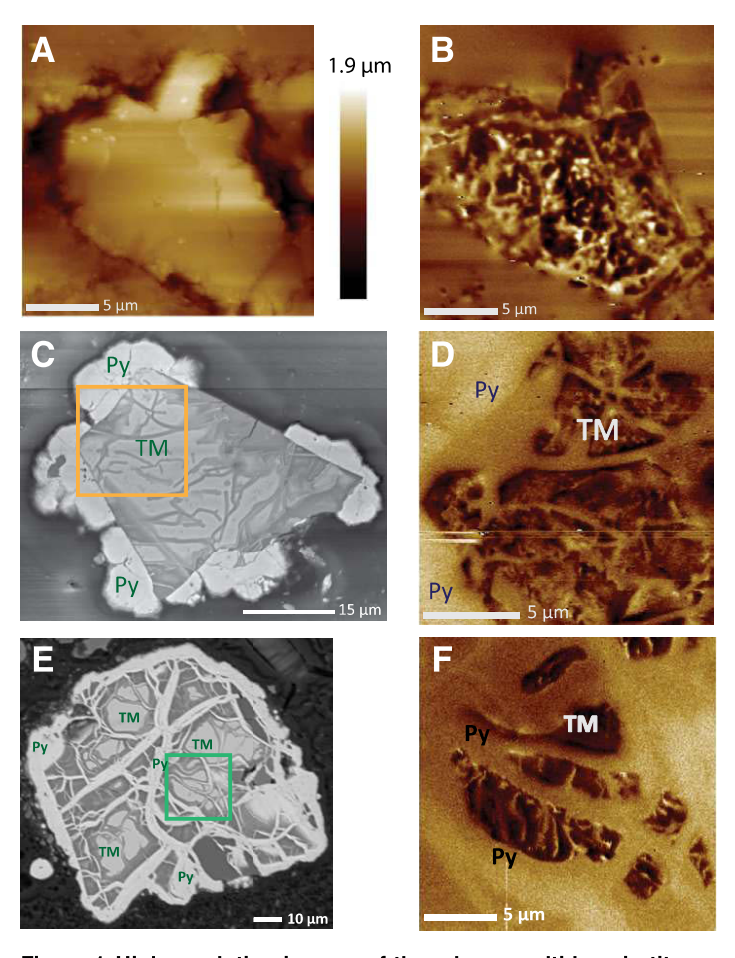


Figure 1. High-resolution images of three large multidomain titanomagnetite grains. A: Topographic map of unaltered titanomagnetite grain from interglacial Holocene. B: Corresponding magnetic phase image. Light and dark patterns are typical of multidomain structures. C: Backscattered electron (BSE) image of partially replaced titanomagnetite (TM) grain with pyrite (Py) rim from glacial Lisan Formation, Dead Sea. D: Magnetic phase image of region indicated by orange square in BSE image. E: BSE image of severely altered titanomagnetite grain from Lisan Formation. F: Magnetic phase image of region bounded by green square, where the alteration process has created isolated subgrains of titanomagnetite surrounded by pyrite. During this process, domain walls must realign, forcing the grain to acquire a new remanent magnetization.

The second type of magnetic grain—noninteracting single domains—was found only in sediments from the glacial Lisan Formation and occurred mainly within pyrite framboids. MFM images of a large, 30 µm pyrite framboid reveal a large number of isolated light and dark pairs (Fig. 2). Each pair comprises a dipole that represents a noninteracting single-domain particle. The single-domain behavior can be demonstrated by imparting an IRM to the sample in two opposing directions. The reversal of the light and dark regions due to the opposite magnetic field direction is typical of single-domain behavior (Shaar and Feinberg, 2013). Electron probe microanalysis (EPMA) results indicate that the grain consists entirely of iron and sulfur, which indicates that the ferrimagnetic mineral responsible for the magnetization is greigite. These greigite inclusions reside within pyrite that has grown around the earlier-formed greigite crystals. To our knowledge, this is the first time that greigite inclusions in pyrite have been observed directly.

The third type of magnetic grain—interacting greigite particles—was found in late Holocene Ze'elim Formation sediments. MFM images contain numerous light and dark pairs that are confined by grain boundaries (Fig. 3). These individual pairs interacted with their neighboring grains to

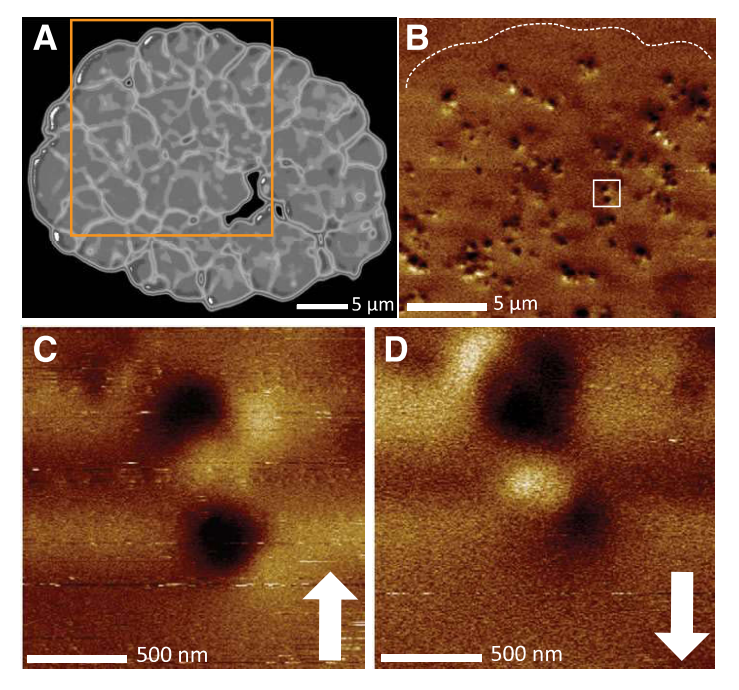


Figure 2. Pyrite framboid containing single-domain greigite inclusions. A: Backscattered electron image of pyrite framboid. B: Magnetic force microscopy (MFM) image of region bounded by orange square, with isolated magnetic domains (light/dark pairs) embedded in pyrite. C–D: Magnified MFM images of region marked by white square with two single-domain–like regions an isothermal remanent magnetization (IRM) has been imparted in opposite directions (indicated by the white arrows).

create larger magnetic aggregates, or a magnetic "superstate" (Harrison et al., 2002), which behaves as a single dipole that is aligned with the direction of the IRM field. This pattern can be demonstrated by reversing the direction of the IRM-producing field, so that the dark and bright pair aggregates switch their directions (Fig. 3). A FORC diagram measured on a bulk sample supports this conclusion: Closed ellipsoidal contours in the

coercivity distribution centered around 60 mT indicate a strong component of interacting single domains (Fig. 3E; Muxworthy et al., 2004; Roberts et al., 2011; Rowan and Roberts, 2006). Additional backscattered images and WDS mapping of grains are provided in the GSA Data Repository¹.

DISCUSSION

"Pyrite Paradox"

The magnetic minerals identified in our study are relevant to the longstanding unresolved "pyrite paradox": why is pyrite, a paramagnetic mineral that has no net spontaneous magnetization, often present in magnetic extracts of lake and marine sediments (Nowaczyk, 2011; Roberts and Turner, 1993; Rowan and Roberts, 2006)? Electron microscopy has a limited ability to resolve small chemical variations, or to identify nanometer-scale greigite grains embedded in larger pyrite crystals. While the presence of greigite has been postulated to account for the magnetism of pyrite (Nowaczyk, 2011), our high-resolution MFM images provide direct evidence of this phenomenon. Moreover, our images of greigite framboids in Holocene samples are consistent with the hypothesis that greigite is a precursor to pyrite (Morse and Cornwell, 1987; Sweeney and Kaplan, 1973; Wilkin and Barnes, 1997). Thus, we infer that the magnetic inclusions within pyrite are relict greigite particles that did not transform into pyrite. The presence of single-domain ferrimagnetic greigite grains within a paramagnetic pyrite can have a dramatic effect on sedimentary magnetism, due to the high-fidelity magnetic recording properties of a noninteracting single domain.

Bacterially Mediated Alteration Overwrites Primary Detrital Magnetic Records

Our findings indicate that as well as being affected by the formation and transformation of sulfide minerals, bacterial alteration of detrital grains during diagenesis could also play an unexpected role in the remanent magnetization of sediments. We propose that mineral alteration could

¹GSA Data Repository item 2018084, additional backscattered images and WDS mapping of grains from the sediment, is available online at http://www.geosociety.org/datarepository/2018/ or on request from editing@geosociety.org.

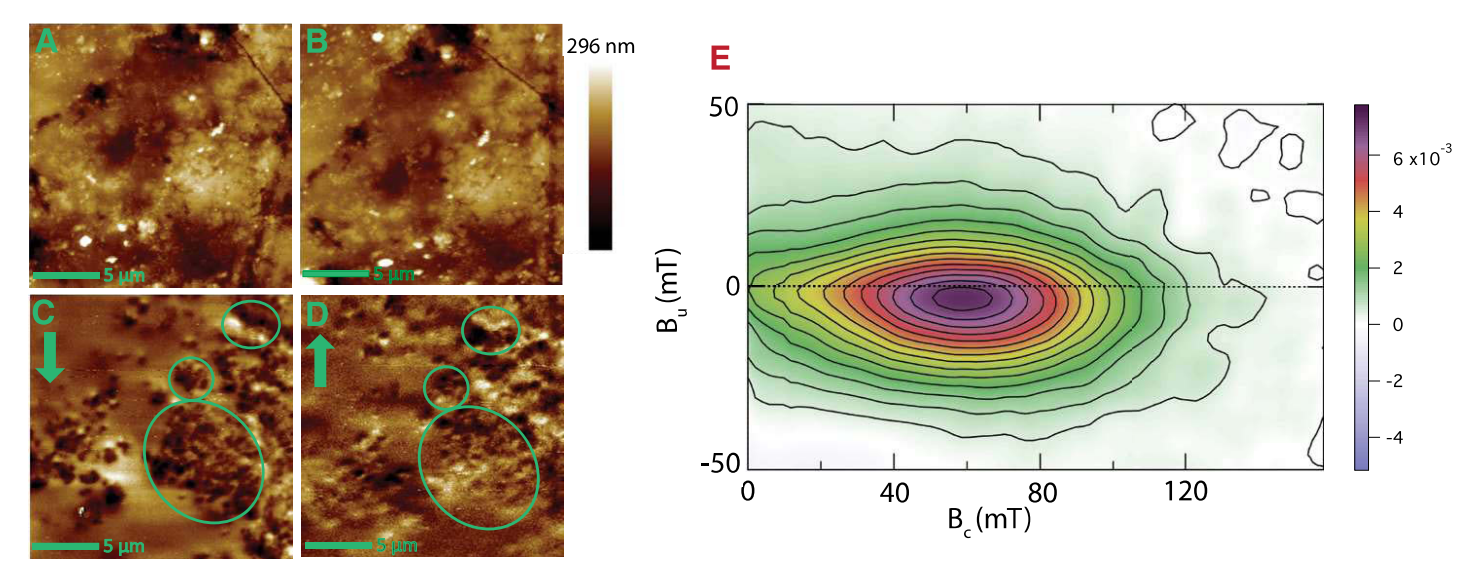


Figure 3. Atomic force microscopy (AFM) and magnetic force microscopy (MFM) images of magnetically interacting greigite aggregates. A–B: Topographic maps of greigite aggregate. C–D: Corresponding magnetic phase images. Topography in the two images indicates clearly that the same region has been scanned; however, the magnetic phase map is different due to the opposing direction of isothermal remanent magnetization (IRM) imparted prior to scanning. Direction of the magnetic field in each case is indicated by the green arrows. Interacting grains respond to the applied field as larger magnetic aggregates, which behave in a similar way to single dipoles. E: First-order reversal curve (FORC) distribution for bulk sediments from the Holocene, interpreted as interacting single-domain greigite. Smoothing factor (SF) = 7, averaging time = 502 ms (Muxworthy et al., 2004; Roberts et al., 2011).

drive a remagnetization process by domain wall realignment. Mineral alteration of the kind we observed in the multidomain grains creates evolving subgrains of different sizes and geometries. As the subgrains change, the magnetic domains must undergo continuous realignment, during which they acquire a secondary magnetic remanence. Thus, mineral replacement of detrital titanomagnetite does not simply erase any primary depositional magnetization carried by the particle; such bacterially mediated processes can overwrite the magnetic signal recorded by detrital grains. However, such remagnetization can only occur as long as the alteration of detrital titanomagnetite particles is incomplete. Crucially, for the overall magnetic signal in sediments, the effective magnetic moment of the secondary magnetization could be larger than the original detrital magnetization because small noninteracting subparticles can have a stronger net magnetization than a single multidomain particle of the same size. Bacterially mediated mineral alteration therefore represents a new pathway for acquisition of secondary magnetizations in sediment.

ACKNOWLEDGMENTS

We thank Ran Issachar for making the first-order reversal curve measurements during a visiting fellowship to the Institute of Rock Magnetism, University of Minnesota (Minneapolis, Minnesota, USA), and to Mike Jackson for assistance. We thank Moshe Eliyahu for assistance with the magnetic force microscopy and Omri Dvir for assistance with the electron probe microanalysis. We thank Andrew Roberts for a helpful and insightful review that significantly improved the paper, and we thank an anonymous reviewer. This study was supported by Israel Science Foundation grant 1364/15 and German-Israeli Foundation (GIF) Young Scientists program grant I-2398–301.8/2015 to Shaar, and the Dead Sea Deep Drill Center of Excellence (COE) of the Israel Science Foundation (grants 1736/11 and 1436/14 to Stein).

We dedicate this paper to the memory of the late Hagai Ron, who initiated the magnetic research of the lacustrine formations of the Dead Sea and made pioneering efforts in understanding the magnetic properties of the unique mineral assemblage that is formed in the lakes.

REFERENCES CITED

- Bartov, Y., Goldstein, S.L., Stein, M., and Enzel, Y., 2003, Catastrophic arid episodes in the Eastern Mediterranean linked with the North Atlantic Heinrich events: Geology, v. 31, p. 439–442, https://doi.org/10.1130/0091-7613(2003) 031<0439:CAEITE>2.0.CO;2.
- Berner, R.A., 1984, Sedimentary pyrite formation—An update: Geochimica et Cosmochimica Acta, v. 48, p. 605–615, https://doi.org/10.1016/0016-7037 (84)90089-9
- Canfield, D.E., and Berner, R.A., 1987, Dissolution and pyritization of magnetite in anoxic marine-sediments: Geochimica et Cosmochimica Acta, v. 51, p. 645–659, https://doi.org/10.1016/0016-7037(87)90076-7.
- de Groot, L.V., Fabian, K., Bakelaar, I.A., and Dekkers, M.J., 2014, Magnetic force microscopy reveals meta-stable magnetic domain states that prevent reliable absolute palaeointensity experiments: Nature Communications, v. 5, p. 4548, https://doi.org/10.1038/ncomms5548.
- Harrison, R.J., Dunin-Borkowski, R.E., and Putnis, A., 2002, Direct imaging of nanoscale magnetic interactions in minerals: Proceedings of the National Academy of Sciences of the United States of America, v. 99, p. 16,556–16,561, https://doi.org/10.1073/pnas.262514499.
- Hunger, S., and Benning, L.G., 2007, Greigite: A true intermediate on the polysulfide pathway to pyrite: Geochemical Transactions, v. 8, p. 1, https://doi .org/10.1186/1467-4866-8-1.
- Morse, J.W., and Cornwell, J.C., 1987, Analysis and distribution of iron sulfide minerals in recent anoxic marine-sediments: Marine Chemistry, v. 22, p. 55–69, https://doi.org/10.1016/0304-4203(87)90048-X.
- Muxworthy, A.R., and Williams, W., 2006, Critical single-domain/multidomain grain sizes in noninteracting and interacting elongated magnetite particles: Implications for magnetosomes: Journal of Geophysical Research–Solid Earth, v. 111, p. B12S12, https://doi.org/10.1029/2006jb004588.
- Muxworthy, A., Heslop, D., and Williams, W., 2004, Influence of magnetostatic interactions on first-order-reversal-curve (FORC) diagrams: A micromagnetic approach: Geophysical Journal International, v. 158, p. 888–897, https://doi. org/10.1111/j.1365-246X.2004.02358.x.
- Neugebauer, I., et al., 2014, Lithology of the long sediment record recovered by the ICDP Dead Sea Deep Drilling Project (DSDDP): Quaternary Science Reviews, v. 102, p. 149–165, https://doi.org/10.1016/j.quascirev.2014.08.013.

- Nowaczyk, N.R., 2011, Dissolution of titanomagnetite and sulphidization in sediments from Lake Kinneret, Israel: Geophysical Journal International, v. 187, p. 34–44, https://doi.org/10.1111/j.1365-246X.2011.05120.x.
- Oren, A., Gurevich, P., Anati, D.A., Barkan, E., and Luz, B., 1995, A bloom of *Dunaliella parva* in the Dead Sea in 1992—Biological and biogeochemical aspects: Hydrobiologia, v. 297, p. 173–185, https://doi.org/10.1007/BF00019283.
- Pokhil, T.G., and Moskowitz, B.M., 1997, Magnetic domains and domain walls in pseudo-single-domain magnetite studied with magnetic force microscopy: Journal of Geophysical Research–Solid Earth, v. 102, p. 22,681–22,694, https://doi.org/10.1029/97JB01856.
- Roberts, A.P., 2015, Magnetic mineral diagenesis: Earth-Science Reviews, v. 151, p. 1–47, https://doi.org/10.1016/j.earscirev.2015.09.010.
- Roberts, A.P., and Turner, G.M., 1993, Diagenetic formation of ferrimagnetic iron sulfide minerals in rapidly deposited marine-sediments, South Island, New Zealand: Earth and Planetary Science Letters, v. 115, p. 257–273, https://doi .org/10.1016/0012-821X(93)90226-Y.
- Roberts, A.P., and Weaver, R., 2005, Multiple mechanisms of remagnetization involving sedimentary greigite (Fe₃S₄): Earth and Planetary Science Letters, v. 231, p. 263–277, https://doi.org/10.1016/j.epsl.2004.11.024.
- Roberts, A.P., Chang, L., Rowan, C.J., Horng, C.S., and Florindo, F., 2011, Magnetic properties of sedimentary greigite (Fe₃S₄): An update: Reviews of Geophysics, v. 49, p. RG1002, https://doi.org/10.1029/2010RG000336.
- Ron, H., Nowaczyk, N.R., Frank, U., Marco, S., and MacWiliams, M.O., 2006, Magnetic properties of Lake Lisan and Holocene Dead Sea sediments and the fidelity of chemical and detrital remanent magnetization, in Enzel, Y., et al., eds., New Frontiers in Dead Sea Paleoenvironmental Research: Geological Society of America Special Paper 401, p. 171–182.
- Rowan, C.J., and Roberts, A.P., 2006, Magnetite dissolution, diachronous greigite formation, and secondary magnetizations from pyrite oxidation: Unravelling complex magnetizations in Neogene marine sediments from New Zealand: Earth and Planetary Science Letters, v. 241, p. 119–137, https://doi.org/10 .1016/j.epsl.2005.10.017.
- Rowan, C.J., Roberts, A.P., and Broadbent, T., 2009, Reductive diagenesis, magnetite dissolution, greigite growth and paleomagnetic smoothing in marine sediments: A new view: Earth and Planetary Science Letters, v. 277, p. 223–235, https://doi.org/10.1016/j.epsl.2008.10.016.
- Sagnotti, L., and Winkler, A., 1999, Rock magnetism and palaeomagnetism of greigite-bearing mudstones in the Italian peninsula: Earth and Planetary Science Letters, v. 165, p. 67–80, https://doi.org/10.1016/S0012-821X(98) 00248-9.
- Shaar, R., and Feinberg, J.M., 2013, Rock magnetic properties of dendrites: Insights from MFM imaging and implications for paleomagnetic studies: Geochemistry Geophysics Geosystems, v. 14, p. 407–421, https://doi.org/10.1002/ggge.20053.
- Stein, M., 2001, The sedimentary and geochemical record of Neogene–Quaternary water bodies in the Dead Sea Basin—Inferences for the regional paleoclimatic history: Journal of Paleolimnology, v. 26, p. 271–282, https://doi.org/10.1023 /A:1017529228186.
- Stein, M., Starinsky, A., Katz, A., Goldstein, S.L., Machlus, M., and Schramm, A., 1997, Strontium isotopic, chemical, and sedimentological evidence for the evolution of Lake Lisan and the Dead Sea: Geochimica et Cosmochimica Acta, v. 61, p. 3975–3992, https://doi.org/10.1016/S0016-7037(97)00191-9.
- Sweeney, R.E., and Kaplan, I.R., 1973, Pyrite framboid formation—Laboratory synthesis and marine sediments: Economic Geology and the Bulletin of the Society of Economic Geologists, v. 68, p. 618–634, https://doi.org/10.2113/gsecongeo.68.5.618.
- Thomas, C., Ebert, Y., Kiro, Y., Stein, M., Ariztegui, D., and the DSDDP Scientific Team, 2016, Microbial sedimentary imprint on the deep Dead Sea sediment: Depositional Record, v. 2, p. 118–138, https://doi.org/10.1002/dep2.16.
- Torfstein, A., Gavrieli, I., and Stein, M., 2005, The sources and evolution of sulfur in the hypersaline Lake Lisan (paleo–Dead Sea): Earth and Planetary Science Letters, v. 236, p. 61–77, https://doi.org/10.1016/j.epsl.2005.04.026.
- Torfstein, A., Goldstein, S.L., Stein, M., and Enzel, Y., 2013, Impacts of abrupt climate changes in the Levant from Last Glacial Dead Sea levels: Quaternary Science Reviews, v. 69, p. 1–7, https://doi.org/10.1016/j.quascirev.2013.02.015.
- Wilkin, R.T., and Barnes, H.L., 1997, Pyrite formation in an anoxic estuarine basin: American Journal of Science, v. 297, p. 620–650, https://doi.org/10.2475/ajs.297.6.620.

Manuscript received 12 September 2017 Revised manuscript received 3 January 2018 Manuscript accepted 3 January 2018

Printed in USA